MOLECULAR AND CELLULAR BIOLOGY, Jan. 2007, p. 554–567 Vol. 27, No. 2
0270-7306/07/$08.00+0 doi:10.1128/MCB.00869-06

Cleavage and Cytoplasmic Relocalization of Histone Deacetylase 3 Are Important for Apoptosis Progression▽†

Fabrice Escaffit,[1] Olivier Vaute,[1] Martine Chevillard-Briet,[1] Bruno Segui,[2] Yasunari Takami,[3] Tatsuo Nakayama,[3] and Didier Trouche[1]*

Laboratoire de Biologie Moléculaire Eucaryote, UMR5099, CNRS and Université Paul Sabatier, IFR109, 118 Route de Narbonne, 31062 Toulouse Cedex 4, France[1]; Laboratoire de Biochimie, Régulations cellulaires, lipidoses et athérosclérose, INSERM U466, IFR31, CHU Rangueil, 1 avenue J. Poulhès, 31403 Toulouse Cedex 4, France[2]; and Section of Biochemistry and Molecular Biology, Department of Medical Sciences, Miyazaki Medical College, University of Miyazaki, 5200, Kihara, Kiyotake, Miyazaki 889-1692, Japan[3]

Received 16 May 2006/Returned for modification 31 July 2006/Accepted 30 October 2006

The apoptotic process is accompanied by major changes in chromatin structure and gene expression. The apoptotic genetic program is progressively set up with the inhibition of antiapoptotic genes and the activation of proapoptotic ones. Here, we show that the histone deacetylase 3 (HDAC-3), which is a known corepressor of many proapoptotic genes, is subjected to proteolytic cleavage during apoptosis in a cell type- and species-independent manner. This cleavage is caspase dependent and leads to the loss of the C-terminal part of HDAC-3. The cleaved form of HDAC-3 accumulates in the cytoplasm. Furthermore, we found that forced nuclear localization of HDAC-3 decreases the efficiency of apoptosis induction, indicating that HDAC-3 cytoplasmic relocalization is important for the apoptotic process. Finally, we observed that HDAC-3 cleavage allowed increased histone acetylation and transcriptional activation on a proapoptotic HDAC-3-target gene, the Fas-encoding gene. Altogether, our results thus indicate that HDAC-3 cleavage is crucial for efficient apoptosis induction because it allows the activation of some proapoptotic genes during apoptosis progression.

Epigenetic marks play a major role in the control of cell fate during mammalian development. Among these, the most studied so far is lysine acetylation, a posttranslational modification of histones which inactivates the positive charge of lysines. Histone hyperacetylation largely correlates with transcription (11). In agreement with this correlation, histone acetyltransferases (HATs) are mostly involved in transcriptional activation, whereas histone deacetylases (HDACs) are often corepressors. The effect of histone acetylation on chromatin function could be mediated by direct effects on nucleosome structure or nucleosome-nucleosome interactions. However, acetylated lysines are also specifically recognized by the so-called "bromodomain," a protein domain present in many chromatin-related proteins (9). The recruitment of activating proteins containing bromodomains to acetylated histones can bring about transcriptional activation (22).

HDAC-3 belongs to the class I histone deacetylase in mammals, which means that its yeast homolog is RPD3. It belongs to a multimolecular complex whose subunits, such as the N-CoR protein, are required for HDAC-3 enzymatic activity (19, 20, 27, 48). HDAC-3 functions as a corepressor for many sequence-specific transcription factors, including NF-κB, E2F/Rb, and c-jun (3, 26, 47, 50). Through a physical interaction with these transcription factors, HDAC-3 is recruited to specific promoters, where it brings about transcriptional repression through histone deacetylation. In addition to this local function, HDAC-3 is also important for global genome-wide histone deacetylation and specific inactivation of HDAC-3 leads to an increase in global histone acetylation (17, 52). Finally, HDAC-3 can also deacetylate nonhistone proteins (6, 8, 42) and it is unclear at this moment whether its role in transcription is mediated though the deacetylation of histones or other transcription factors.

Little is known about HDAC-3 regulation. Recently, it was shown that its activity is regulated by protein phosphatase 4 (51). Moreover, HDAC-3 possesses a unique property among class I HDACs, localizing in both the cytoplasm and the nucleus (3, 16, 50). Indeed, it contains a nuclear localization signal (NLS) at its C terminus and two different nuclear export sequences have been proposed (40, 50). Moreover, its subcellular localization is known to be regulated through a physical interaction with Tab2, which induces HDAC-3 relocalization to the cytoplasm following interleukin-1β treatment (3).

Importantly, HDAC-3 seems to be critical for the control of apoptosis. Many transcription factors regulated by HDAC-3 are important for apoptosis, including NF-κB and E2F (3, 26, 47, 50). Moreover, the inactivation of HDAC-3 in chicken or mammalian cells leads to apoptosis induction (17, 40) or favors apoptosis (33).

Specific modifications of chromatin are likely to play an important role in apoptosis control. Indeed, the induction of histone hyperacetylation using HDAC inhibitors is often sufficient to induce apoptosis (30). Apoptosis is characterized by major changes in chromatin structure since chromatin is highly compacted and DNA is extensively cleaved. Recent data have shown that apoptosis is accompanied by global changes in

* Corresponding author. Mailing address: Laboratoire de Biologie Moléculaire Eucaryote, UMR5099, CNRS and Université Paul Sabatier, IFR109, 118 Route de Narbonne, 31062 Toulouse Cedex 4, France. Phone: 33 5 61 33 59 15. Fax: 33 5 61 33 58 86. E-mail: trouche@ibcg.biotoul.fr.

† Supplemental material for this article may be found at http://mcb.asm.org/.

▽ Published ahead of print on 13 November 2006.

histone modifications, such as phosphorylation or ubiquitination (1, 7, 25, 32, 36, 41). Moreover, the activation of proapoptotic genes and the inactivation of antiapoptotic genes, which occur during apoptosis, are accompanied by specific changes in histone modifications at these promoters. Correspondingly to this wave of changes in histone modifications, the activity of many proteins modifying histones is affected during apoptosis, mostly through caspase-mediated cleavage (2, 4, 39). Concerning enzymes controlling histone acetylation levels, it has been observed that the HAT CBP/p300 is cleaved during apoptosis in the central nervous system, leading to the loss of its HAT activity (37). Recently, another histone deacetylase, HDAC-4, has also been shown to be a substrate of caspases (34).

Because of the role of HDAC-3 in apoptosis control, we investigated its regulation during apoptosis. We found that HDAC-3 is cleaved during apoptosis, and we demonstrate that this cleavage may participate in the establishment of the apoptotic genetic program.

MATERIALS AND METHODS

Cell culture and transfection. Jurkat cells and derivatives were cultured in RPMI supplemented with antibiotics and fetal calf serum (FCS) (10%). DT40 and ΔchHDAC3/FHDAC-3 cells were cultured in RPMI supplemented with antibiotics, FCS (10%), chicken serum (1%), and β-mercaptoethanol (10 μM). U2OS cells were cultured in Dulbecco's modified Eagle's medium (DMEM) supplemented with antibiotics and FCS (10%). All materials were from Invitrogen (Invitrogen Life Technologies, Carlsbad, CA). For UV irradiation, nonadherent cells were collected, washed with phosphate-buffered saline (PBS), and resuspended in PBS (50 μl for 10^6 cells). Cells were then spotted in a petri dish to obtain a monolayer. Irradiation was performed using a UV cross-linker (Hoefer). Adherent cells were washed with PBS, and irradiation was performed similarly. Warm culture medium was then added. Other apoptosis-inducing treatments were performed using staurosporine (Sigma-Aldrich, Saint Louis, MO) or Fas ligand (FasL)-containing cell supernatant prepared as described previously (38). Doxycycline (BD Biosciences, Mountain View, CA) was used at a concentration of 100 ng/ml. Z-VAD (Sigma) was used at a concentration of 50 μM. The transfection of small interfering RNA (siRNA) was performed by electroporation using a Gene Pulser Xcell apparatus (Bio-Rad Laboratories, Hercules, CA) according to the manufacturer's instructions using 10 μl of siRNA (100 μM) for 5×10^6 cells.

siRNA and antibodies. The sequences of the top strand of siRNAs (all from Eurogentec) were as follows: for the control, CAUGUCAUGUGUCACAUC U-dTdT; for anti-HDAC-3 S1, CGACAUUGUGAUUGGCAUC-dTdT; and for anti-HDAC-3 S2, GAUGCUGAACCAUGCACCU-dTdT. Anti-HDAC-3 antibodies were purchased from Transduction Laboratories, Upstate Biotechnology, or Santa Cruz Biotechnology. The anti-cleaved PARP [poly(ADP) ribose polymerase] antibody was from Promega Corporation (Madison, WI), and the anti-PARP antibody (recognizing both forms of PARP) was from Cell Signaling Technology. Anti-acetylated histone antibodies were all from Upstate Biotechnology. Anti-hemagglutinin (HA) and anti-Flag M2 antibodies were purchased from Covance and Sigma, respectively. Anti-histone H3 antibody was a kind gift from S. Müller (Strasbourg, France). The anti-Rb antibody (clone G3-245) was from Becton Dickinson-Pharmingen.

Cell extracts and Western blotting. For total cell lysates, cells were washed in PBS and total proteins were extracted using the lysis buffer containing Triton X-100 (1%), sodium dodecyl sulfate (SDS) (2%), NaCl (150 mM), phosphatases, and proteases inhibitors in Tris-HCl 100 mM, pH 7.4. Total cell extracts were quantified using a DC protein assay kit from Bio-Rad, and 10 μg of proteins per lane were separated by SDS-polyacrylamide gel electrophoresis. Gels were transferred using a Bio-Rad apparatus on a nitrocellulose membrane. Western blot analyses were performed by standard procedures using peroxidase-conjugated secondary antibodies. Peroxidase was then detected by using the LumiLight-plus reagent (Roche Diagnostics, Meylan, France).

For cell fractionation, a previously described protocol (10) was used with modifications. Briefly, 10^8 cells for each condition were harvested, washed in PBS, and resuspended in cell hypotonic lysis buffer containing 10 mM HEPES, pH 7.9, 1.5 mM $MgCl_2$, 10 mM KCl, 0.5 mM dithiothreitol (DTT), and protease inhibitors. After incubation on ice for 10 min and centrifugation, the supernatant (hypotonic lysis fraction) was collected. Then, the resuspension-incubation step was repeated three times. Centrifugation at 15,000 × *g* for 20 min was then performed to pellet the nuclei, which were resuspended in an hypertonic buffer containing 20 mM HEPES, pH 7.9, 25% glycerol, 0.42 M NaCl, 1.5 mM $MgCl_2$, 0.2 mM EDTA, 0.5 mM DTT, and protease inhibitors. During the incubation of samples on ice for 30 min, chromatin was scratched frequently using syringes. After the centrifugation, the supernatant (high-salt extracts) was dialyzed for 1 h against 50 volumes of a solution containing 20 mM HEPES, pH 7.9, 20% glycerol, 0.1 M KCl, 0.2 mM EDTA, 0.5 mM DTT, and protease inhibitors.

Apoptosis assay using flow cytometry. Cells were harvested by centrifugation and treated using an annexin V-fluorescein isothiocyanate (FITC)/7-amino-actinomycin D (AAD) kit (Beckman Coulter, Marseille, France) according to the manufacturer's instructions. Cells were then analyzed by flow cytometry, and the percentage of cells with high annexin V expression and that were negative for 7-AAD (representing apoptotic cells) was measured.

RNA extraction, reverse transcription, and ChIP assay. cDNA preparation and chromatin immunoprecipitation (ChIP) assays were performed essentially as described previously (44). For ChIPs, the amounts of *fas* promoter and glyceraldehyde-3-phosphate dehydrogenase (GAPDH) were analyzed by quantitative PCR (Q-PCR). In all experiments, the amounts present in the control immunoprecipitates were negligible.

Q-PCR analysis. Q-PCR analysis was performed on an iCycler device (Bio-Rad) using the platinum SYBR green qPCR SuperMix (Invitrogen). All experiments included a standard curve. All samples were analyzed in triplicate, and the mean and standard deviation were calculated. The following primer pairs were used to amplify cDNAs after reverse transcription experiments: for HDAC-3, CATAGCCTGGTCCTGCATTA and AGTCATCGCCTACGTTG AAG; for ribosomal phosphoprotein P0, GGCGACCTGGAAGTCCAACT and CCATCAGCACCACAGCCTTC; for *fas*, ATGCCCAAGTGACTGACATC and ATGATGCAGGCCTTCCAAGT; and for *bax*, GATGATTGCCGCCGTG GACA and GCACCAGTTTGCTGGCAAAG.

The following primer pairs were used to amplify genomic DNA from ChIPs: for the *fas* promoter, TCTCGAGGTCCTCACCTGAA and TTGGGGAGGG CTCCATTGAT, and for the GAPDH promoter, GAAGGTGAAGGTCGGA GTCA and GAAGATGGTGATGGGATTTC.

Construction of the U2OS R_{BHEN}^{HDAC-3} cell line. The cDNA encoding the full-length human HDAC-3 was cloned into the retroviral pBabe vector, in fusion with the HA-tagged ligand binding domain of the estrogen receptor (HA-ER) and a consensus NLS. The HA-ER encoding vector was a kind gift from K. Helin (Copenhagen, Denmark). The details of construction are available on request. The HA-ER-NLS-HDAC-3-coding vectors were used to produce viruses in GP293 cells by cotransfections with the helper pantropic vector pVPackVSV-G (BD Biosciences). A total of 5×10^6 to 8×10^6 GP293 cells (BD Biosciences) were transfected overnight by using a FuGENE transfection kit (Roche Diagnostics). Cell culture medium (DMEM; Invitrogen Life Technologies) was collected 48 h after transfection and filtered through Millex-HA filters (25 mm, 0.45 μm; Sartorius). Subconfluent U2OS cells were infected with a viral suspension containing 4 μg/ml of Polybrene (hexadimethrine bromide H-9268; Sigma-Aldrich) for 1 h at 37°C with agitation. The medium was then changed, and selection for puromycin (1.0 μg/ml; Invitrogen Life Technologies) resistance was applied 48 h later for 10 days in order to obtain stable U2OS R_{BHEN}^{HDAC-3} populations. Nuclear translocation of the chimera was induced using 300 nM OHTam.

DAPI staining and immunofluorescence. Cells were grown on glass coverslips at 37°C. After brief washes with PBS, cells were fixed in 2% paraformaldehyde (Sigma-Aldrich) in PBS for 45 min at room temperature, permeabilized with 1% Triton in PBS for 5 min and quenched 45 min at 4°C in 0.75% glycine (Roche Diagnostics) in PBS. Cells were blocked in 1% bovine serum albumin in PBS for 30 min and incubated for 1 h with primary antibodies diluted in the blocking solution (Covance), washed three times for 10 min with PBS, incubated with fluorescein isothiocyanate- or rhodamine-conjugated secondary antibodies (Chemicon International, Inc.), stained with DAPI (4′,6′-diamidino-2-phenylindole), washed extensively in PBS, and mounted in Vectashield mounting medium (Vector Laboratories, Burlingame, CA). Observations were carried out with a fluorescence microscope (DM; Leica, Wetlar, Germany) or a phase-contrast microscope equipped with a cooled charge-coupled-device camera, and the acquisition of native images was carried out using the MetaVue imaging system (Universal Imaging Corp., West Chester, PA).

RESULTS

HDAC-3 is subjected to proteolytic cleavage during apoptosis. Apoptosis is accompanied by major changes in chromatin

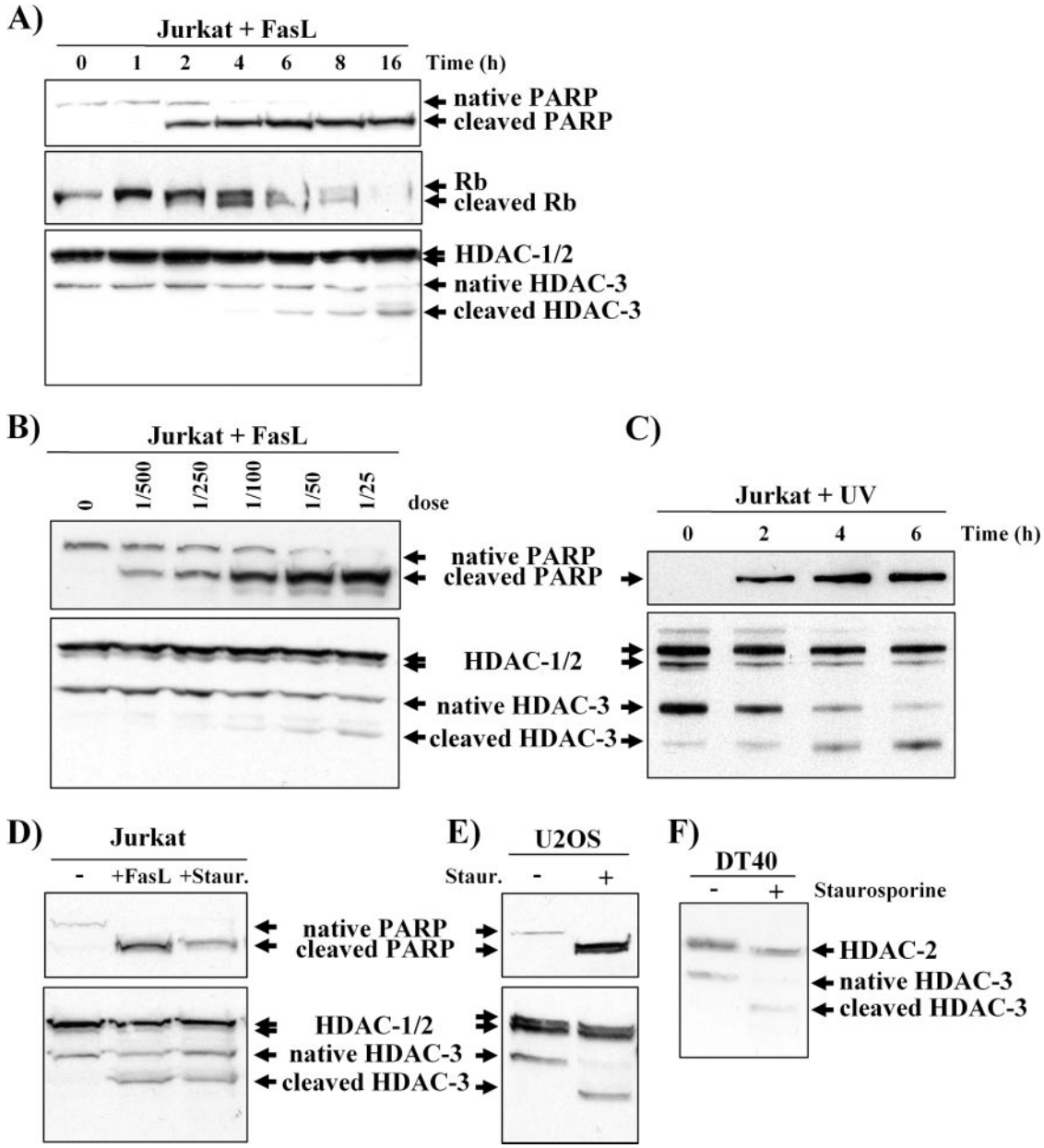

FIG. 1. Cleavage of HDAC-3 during apoptosis. (A) Jurkat T cells were treated with FasL (1/50 dilution of FasL-containing cell supernatant) and harvested after the indicated time. Total cell extracts were prepared, and 10 μg was analyzed by Western blotting using an anti-PARP antibody (detecting both full-length [native PARP] and caspase-cleaved PARP [cleaved PARP] [top panel]), an anti-Rb antibody (middle panel), and an anti-HDAC-3 antibody (from Transduction Laboratories, also recognizing HDAC-1 and HDAC-2 [bottom panel]). (B) Same as described for panel A, except that Jurkat cells were treated for 16 h with the indicated dilution of FasL-containing supernatant. (C) Same as described for panel A, except that Jurkat cells were UV irradiated (40 J/m^2) and harvested after the indicated time. PARP cleavage was monitored using an antibody recognizing only p85 cleaved PARP. (D) Same as described for panel A, except that Jurkat cells were treated by FasL (1/25 dilution) or staurosporine (250 nM) for 16 h. (E) Same as described for panel A, except that U2OS osteosarcoma cells were treated with staurosporine (250 nM) for 16 h. (F) DT40 chicken B cells were treated with staurosporine (250 nM) for 16 h. Total cell extracts were prepared and analyzed by Western blotting using an anti-HDAC-3 antibody (from Transduction Laboratories) also recognizing chicken HDAC-2. −, absence of; +, presence of.

structure, including chromatin condensation and DNA cleavage. Chromatin modifications and chromatin-modifying enzymes are thus susceptible to playing an important role in apoptosis control. We thus investigated the expression of three class I HDACs during the apoptosis of Jurkat cells, a tumoral human T-lymphocyte cell line. We treated cells with FasL, which induces apoptosis through the Fas death receptor pathway. Apoptosis was monitored by the appearance of the caspase-dependent cleaved form of PARP (Fig. 1A, top panel). By Western blot analysis using an anti-HDAC-3 antibody which recognizes HDAC-1, -2, and -3, we found that following apoptosis induction, HDAC-3 expression strongly

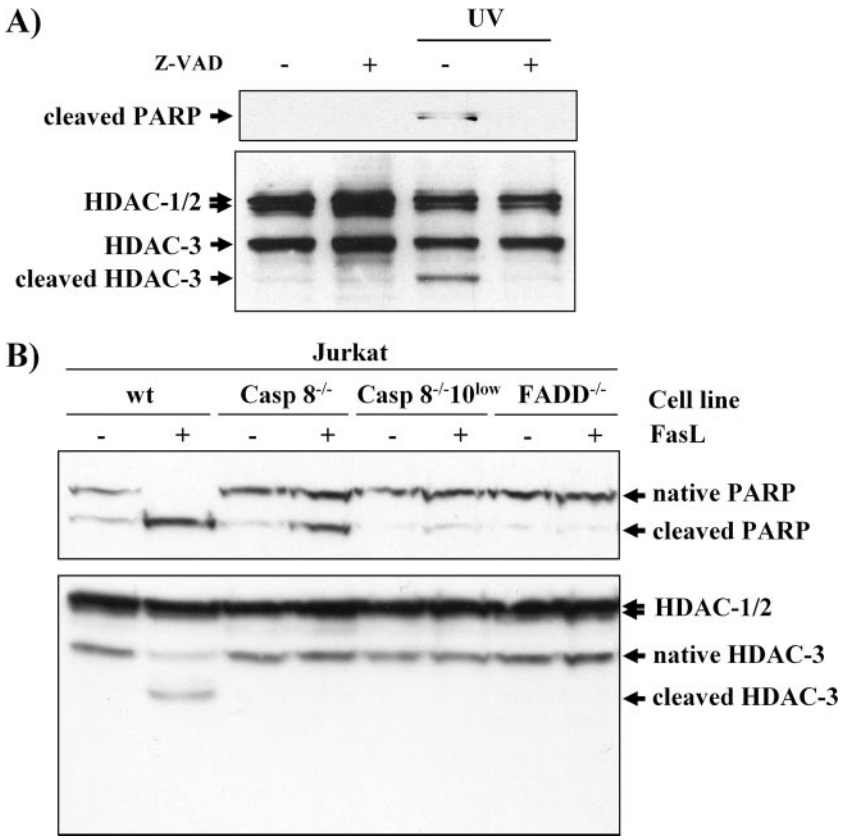

FIG. 2. HDAC-3 cleavage is caspase dependent. (A) Jurkat cells were treated or not treated with Z-VAD (50 μM) as indicated. Two hours later, cells were then UV irradiated (40 J/m^2) as indicated and harvested 4 h later. Total cell extracts were then analyzed by Western blotting using an anti-cleaved PARP antibody (upper panel) and an anti-HDAC-3 antibody (from Transduction Laboratories, lower panel). (B) Jurkat cells with the indicated signaling defects were treated with FasL (1/50 dilution) and harvested 16 h later. Total cell extracts were prepared, and 10 μg was analyzed by Western blotting using an anti-PARP antibody (detecting both full-length [native PARP] and caspase-cleaved PARP [cleaved PARP] [top panel]) and an anti-HDAC-3 antibody (from Transduction Laboratories, also recognizing HDAC-1 and HDAC-2 [bottom panel]). −, absence of; +, presence of.

decreased, whereas HDAC-1 and -2 expression levels did not vary (Fig. 1A, bottom panel). Concomitantly to the HDAC-3 decrease, the apparition of a faster-migrating band could be observed, suggesting that the decrease in HDAC-3 expression was due to proteolytic cleavage of HDAC-3. In agreement with this interpretation, we could also observe such a similar faster-migrating band using recombinant HDAC-3 (see Fig. S1 and S2 in the supplemental material). Moreover, this band was immunodepleted by an HDAC-3-specific antibody (see Fig. S3 in the supplemental material), demonstrating that it is derived from HDAC-3. Thus, the faster-migrating band detected by the anti-HDAC-3 antibody is from now on referred as "cleaved HDAC-3." HDAC-3 cleavage following apoptosis induction by FasL is both time and concentration dependent (Fig. 1A and B). The quantification of the experiment represented in Fig. 1A indicates that the kinetics of the disappearance of full-length PARP and full-length HDAC-3 were very similar (see Fig. S4 in the supplemental material). Moreover, cleavage of HDAC-3 was parallel to the caspase-mediated cleavage of the retinoblastoma protein Rb (Fig. 1A). Taken together, these two sets of data indicate that HDAC-3 cleavage was roughly concomitant to effector caspase activation.

We further found that HDAC-3 cleavage could also be observed when apoptosis was induced by DNA damage (Fig. 1C) or by staurosporine (Fig. 1D), an inhibitor of protein kinase C which induces the release of cytochrome *c* from mitochondria. Since these two latter treatments induce apoptosis through the mitochondrial pathway, these results indicate that HDAC-3 cleavage is a general feature of apoptosis in Jurkat cells. Moreover, HDAC-3 was also cleaved when U2OS human osteosarcoma cells (Fig. 1E) or DT40 chicken lymphoid cells (Fig. 1F) were induced to apoptosis following staurosporine treatment, indicating that HDAC-3 cleavage is neither T lymphocyte specific nor species specific and is thus likely to be a general hallmark of apoptosis.

HDAC-3 cleavage is caspase dependent. Apoptosis is characterized by the activation of specific proteases, called caspases, which control the progression towards programmed cell death. To check whether caspases are involved in HDAC-3 cleavage, we treated Jurkat cells with the caspase inhibitor Z-VAD prior to apoptosis induction. We observed that Z-VAD treatment led to the inhibition of PARP cleavage, which was expected since PARP cleavage is mediated by caspase 3. HDAC-3 cleavage was also inhibited (Fig. 2A), suggesting that caspase activity is required for HDAC-3 cleavage. Because chemical inhibitors may inhibit pathways other than the rele-

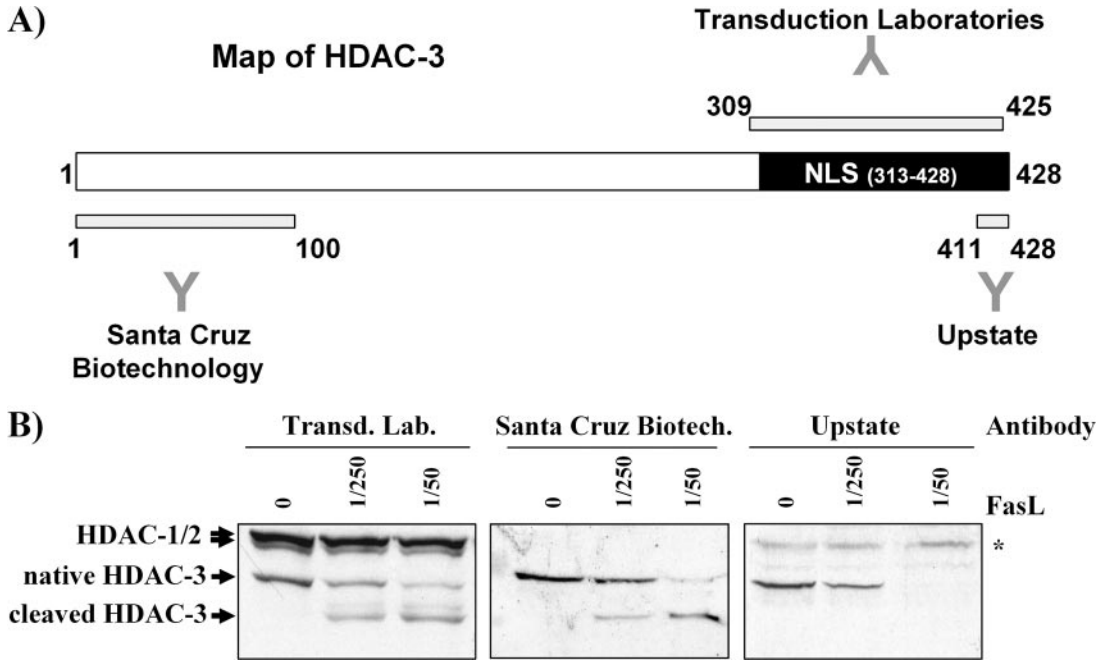

FIG. 3. HDAC-3 is cleaved at its C terminus. (A) Schematic representation of mammalian HDAC-3. The putative NLS is indicated. Also shown are the locations of the epitopes of the various antibodies used for panel B. (B) Jurkat cells were treated with the indicated dilution of FasL-containing cell supernatant and harvested 16 h later. Total cell extracts were prepared, and 10 μg was analyzed by Western blotting using an antibody directed against the N terminus of HDAC-3 (from Santa Cruz Biotechnology), the last 116 amino acids of HDAC-3 (from Transduction Laboratories, also recognizing HDAC-1 and HDAC-2), and the last 18 amino acids of HDAC-3 (from Upstate Biotechnology). The asterisk indicates a nonspecific band detected by the Upstate antibody.

vant ones, we also made use of Jurkat cells mutated in central elements of the pathways leading to effector caspase activation during Fas-induced apoptosis (31). We found that HDAC-3 cleavage following FasL treatment was dependent both on FADD, a protein responsible for signal transduction from the Fas receptor, and on initiator caspase 8 expression since no or very little cleavage was observed in cells deficient for FADD or caspase 8 (Fig. 2B). Thus, taken together, these results indicate that HDAC-3 cleavage during apoptosis is dependent upon caspase activation.

HDAC-3 cleavage leads to the loss of its C terminus. We next wanted to characterize which part of HDAC-3 is absent in its cleaved form. According to its migration in SDS-polyacrylamide gel electrophoresis, cleaved HDAC-3 seemed to be about 7 to 8 kDa smaller than uncleaved HDAC-3, which could result from the loss of between 40 to 70 amino acids. The antibody from Transduction Laboratories that we used in the previous experiments was raised against the C-terminal 126 amino acids of HDAC-3 (Fig. 3A). Moreover, since it also recognizes HDAC-1 and HDAC-2, its epitope is likely to lie between amino acids 309 and 317. Thus, using this antibody, we may not discriminate between a C-terminal cleavage and an N-terminal cleavage. In order to precisely map the proteolytic site, we tested the abilities of other HDAC-3 antibodies to recognize the cleaved form of HDAC-3. Using an antibody directed against the last 17 amino acids of HDAC-3 (Upstate Biotechnology), we efficiently detected full-length HDAC-3 but not cleaved HDAC-3 (Fig. 3B), indicating that HDAC-3 cleavage resulted in the loss of this epitope. Moreover, an antibody directed against the N-terminal 20 amino acids of HDAC-3 (Santa Cruz Biotechnology) recognized both uncleaved and cleaved HDAC-3 (Fig. 3B). Finally, we found that cleaved recombinant HDAC-3 was also detected using an antibody directed against an N-terminal Flag tag (see Fig. S2 in the supplemental material). Thus, altogether, these results indicate that HDAC-3 cleavage results in a protein devoid of its C terminus.

Cleavage of HDAC-3 resulted in its cytoplasmic relocalization. The C-terminal end of HDAC-3 is required for its nuclear localization (50). We thus investigated whether the cleavage of HDAC-3 resulted in a change in the subcellular localization of HDAC-3. We treated Jurkat cells with Fas ligand in order to achieve approximately 50% cleavage, and we prepared cytoplasmic extracts by hypotonic lysis. We found that these cytoplasmic extracts were only weakly contaminated by nuclear proteins since HDAC-1 and HDAC-2, which are mainly nuclear, were present at very low levels in this fraction (Fig. 4A). We found that cleaved HDAC-3 was greatly enriched in this cytoplasmic fraction, whereas it was largely absent in high-salt extracts containing mostly nuclear proteins (Fig. 4A). In contrast, full-length, uncleaved HDAC-3 was found predominantly in the high-salt extracts. This experiment thus suggests that cleaved HDAC-3, in contrast to uncleaved HDAC-3, is mainly cytoplasmic.

Since the late stages of apoptosis are accompanied by the permeabilization of the nuclear envelope, which could lead to apparent cytoplasmic localization of an extractible nuclear protein in fractionation experiments, we also performed immunofluorescence studies. We used the HDAC-3 antibody from Santa Cruz Biotechnology, which recognizes both forms of

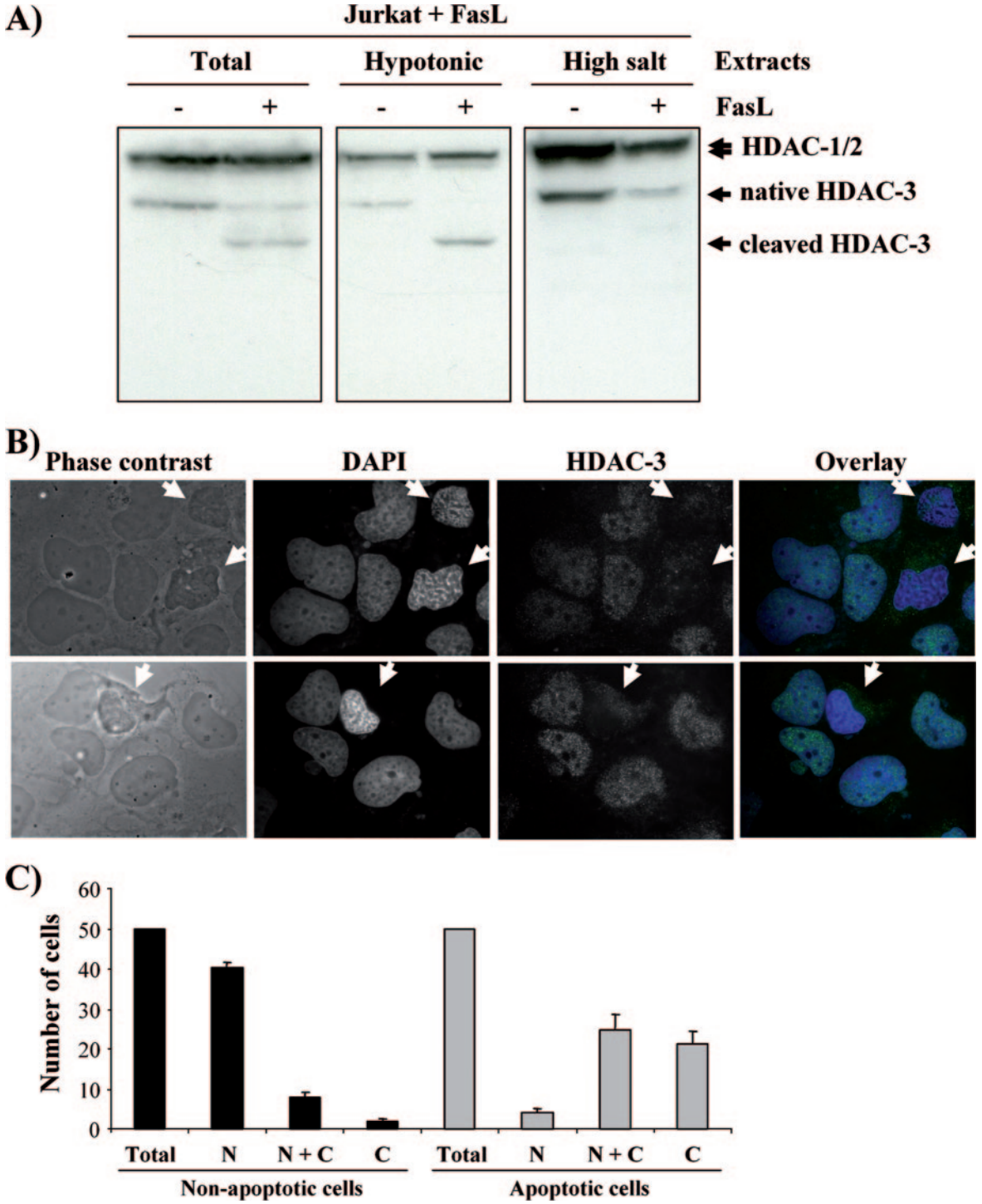

FIG. 4. Cleaved HDAC-3 accumulates in the cytoplasm. (A) Jurkat cells treated with FasL-containing cell supernatant for 16 h were harvested and subjected to fractionation as described in Materials and Methods. Twenty micrograms of total cell extracts (left panel), the hypotonic lysis fraction (middle panel), or high-salt extracts (right panel) were analyzed by Western blotting using an anti-HDAC-3 antibody (from Transduction Laboratories, also recognizing HDAC-1 and HDAC-2). −, absence of; +, presence of. (B) U2OS cells were irradiated with UV (40 J/m^2) and subjected to immunofluorescence staining 6 h later using the anti-HDAC-3 antibody from Santa Cruz Biotechnology. Also shown are phase-contrast microscopy, DAPI staining, and the overlay of DAPI and anti-HDAC-3 stainings. Two different representative fields are shown. The arrows point to apoptotic cells. (C) Quantification of the experiment represented in panel B. Fifty nonapoptotic or apoptotic cells (according to DAPI staining) were analyzed for HDAC-3 staining. The graph represents the means and standard deviations (error bars) from four independent fields. N, nuclear only; C, cytoplasmic only; N+C, nuclear and cytoplasmic.

HDAC-3 (Fig. 3). In nonapoptotic U2OS cells, this antibody stained mainly the nucleus as small dots (Fig. 4B). This nuclear staining reflected the recognition of endogenous HDAC-3 since costaining with another anti-HDAC-3 antibody (Upstate Biotechnology), which recognizes only uncleaved HDAC-3 (Fig. 3), showed perfect colocalization (data not shown). In cells undergoing apoptosis (Fig. 4B), as indicated by phase-contrast microscopy and DAPI staining monitoring chromatin condensation, nuclear HDAC-3 staining was no longer observed, whereas cytoplasmic staining strongly increased. The quantification of this experiment (Fig. 4C) indeed confirmed that whereas HDAC-3 was exclusively nuclear in most cells before apoptosis induction, it was either exclusively cytoplasmic or observed throughout the cell in apoptotic cells. Altogether, these results indicate that following apoptosis induction, HDAC-3 is cleaved and relocalized to the cytoplasm.

Inhibition of HDAC-3 favors apoptosis. Results from the above experiments indicate that, in apoptotic cells, HDAC-3 is mainly localized in the cytoplasm. Obviously, once in the cytoplasm, HDAC-3 is unable to deacetylate nucleosomal histones, indicating that the cleavage of HDAC-3 results in the inactivation of HDAC-3 deacetylase activity towards histones. In order to test whether the inhibition of HDAC-3 could be important for apoptosis induction, we transfected U2OS cells with two HDAC-3 specific siRNAs. Surprisingly, whereas both siRNAs similarly decreased HDAC-3 expression (see Fig. 7A for an example), they had opposite effects on apoptosis induction (data not shown). This result could be due to the existence of various HDAC-3 isoforms that would not be similarly targeted by the two siRNAs. Indeed, alternative splicing of HDAC-3 mRNA has already been described (18). Note, however, that we cannot rule out the possibility that one of the two siRNAs exhibited "off target" effects. Thus, to clarify the role of HDAC-3 in apoptosis, we used an inducible knockout system raised in chicken DT40 cells by Takami and Nakayama (40). Indeed, we already observed that apoptosis induction in DT40 cells was also accompanied by HDAC-3 cleavage (Fig. 1). Thus doxycycline was added or not to DT40 cells harboring the inducible HDAC-3 transgene, and we found that, as expected, the doxycycline addition led to the rapid disappearance of HDAC-3 since virtually no protein could be detected after 2 days of treatment (Fig. 5A). We then added staurosporine to these cells, and we compared the efficiency of apoptosis induction in HDAC-3-expressing cells to that in nonexpressing cells by annexin V/7-AAD staining (PARP cleavage could not be assessed in these cells since anti-PARP antibodies did not recognize chicken PARP [data not shown]). We found that HDAC-3 inhibition for 2 days had no effect by itself on apoptosis induction (Fig. 5B), as already shown (40). However, doxycycline-treated cells were more sensitive to staurosporine-induced apoptosis, indicating that knockdown of HDAC-3 favors apoptosis induction. Thus, altogether, our results indicate that the proteolytic cleavage of HDAC-3 could favor apoptosis by decreasing the nuclear levels of HDAC-3, thereby inhibiting HDAC-3-mediated histone deacetylation.

Forced nuclear localization of HDAC-3 inhibits apoptosis. To test this possibility, we set up a system in which the expression of HDAC-3 can be artificially forced in the nucleus. We transduced U2OS cells (in which we had already observed HDAC-3 cleavage [Fig. 1]) with a retroviral vector, allowing the expression of a chimeric protein in which a mutated version of the ligand binding domain of the estrogen receptor is fused to the N terminus of HDAC-3 (ER-HDAC-3). This fusion protein also contains an HA epitope and a NLS from the simian virus 40 T antigen. Similar fusion proteins between this ER ligand binding domain and the E2F or c-*myc* transcription factors have already been widely used (28, 45). These chimeric proteins are cytoplasmic in the absence of OHTam (hydroxytamoxifen) and become nuclear upon the addition of OHTam. We first checked that the ER-HDAC-3 fusion protein behaved as expected. By immunofluorescence using the anti-HA antibody, we found that, in absence of OHTam, the fusion protein was mainly cytoplasmic, whereas very rapidly upon OHTam addition, the fusion protein became nuclear (Fig. 6A). Thus, the addition of OHTam allowed the forced nuclear localization of ER-HDAC-3. We thus investigated how the presence of nuclear ER-HDAC-3-affected apoptosis induction in these cells. These cells were treated or not treated with OHTam, and we irradiated them with UV in order to induce apoptosis. Surprisingly, the fusion protein did not seem to be cleaved following apoptosis induction, certainly because the ER tag prevented it from being recognized by apoptosis-induced proteases (Fig. 6B). We observed that apoptosis induction, as indicated by PARP cleavage, was less efficient in the presence of OHTam than in its absence (Fig. 6B). This decrease was most likely due to a lower number of cells undergoing apoptosis, as indicated by the analysis of cells harboring apoptotic-related chromatin condensation (Fig. 6C and D). Importantly, such an effect was not observed using the parental U2OS cell line (data not shown). These results demonstrate that the forced nuclear localization of ER-HDAC-3 inhibits apoptosis. We cannot rule out the possibility that this decrease in apoptosis is due to HDAC-3 overexpression and the titration of a caspase or an apoptosis-related protease. However, such a possibility is unlikely since HDAC-3 overexpression is not massive. Indeed, ER-HDAC-3 expression is comparable to that of endogenous HDAC-3 (see Fig. S5 in the supplemental material). Therefore, our results suggest that the decrease in HDAC-3 nuclear levels induced by its cleavage is important for efficient apoptosis induction.

Analysis of global histone acetylation upon apoptosis induction. We next intended to investigate the consequence of HDAC-3 cleavage on histone acetylation. We first tested whether apoptosis induction would be accompanied by increased global histone acetylation at HDAC-3 target lysines. Indeed, HDAC-3 has already been proposed to be a major histone deacetylase in mammalian cells (14, 17, 52). Moreover, histone deacetylase inhibitors, which induced global histone hyperacetylation, also favored UV-induced apoptosis in U2OS cells (see Fig. S6 in the supplemental material). We first intended to characterize HDAC-3 target lysines by siRNA-mediated knockdown of HDAC-3. Although our two anti-HDAC-3 siRNAs had opposite effects on apoptosis, they can be used to study HDAC-3 direct targets. The transfection of U2OS cells with these two siRNAs led to the decrease of HDAC-3 expression, both at the mRNA level and the protein level (Fig. 7A). We first analyzed global histone acetylation by Western blotting using antibodies specific for acetylated histones. In similar experimental settings, HDAC-3 has already been found to deacetylate mainly K9 of histone H3 and K5 of

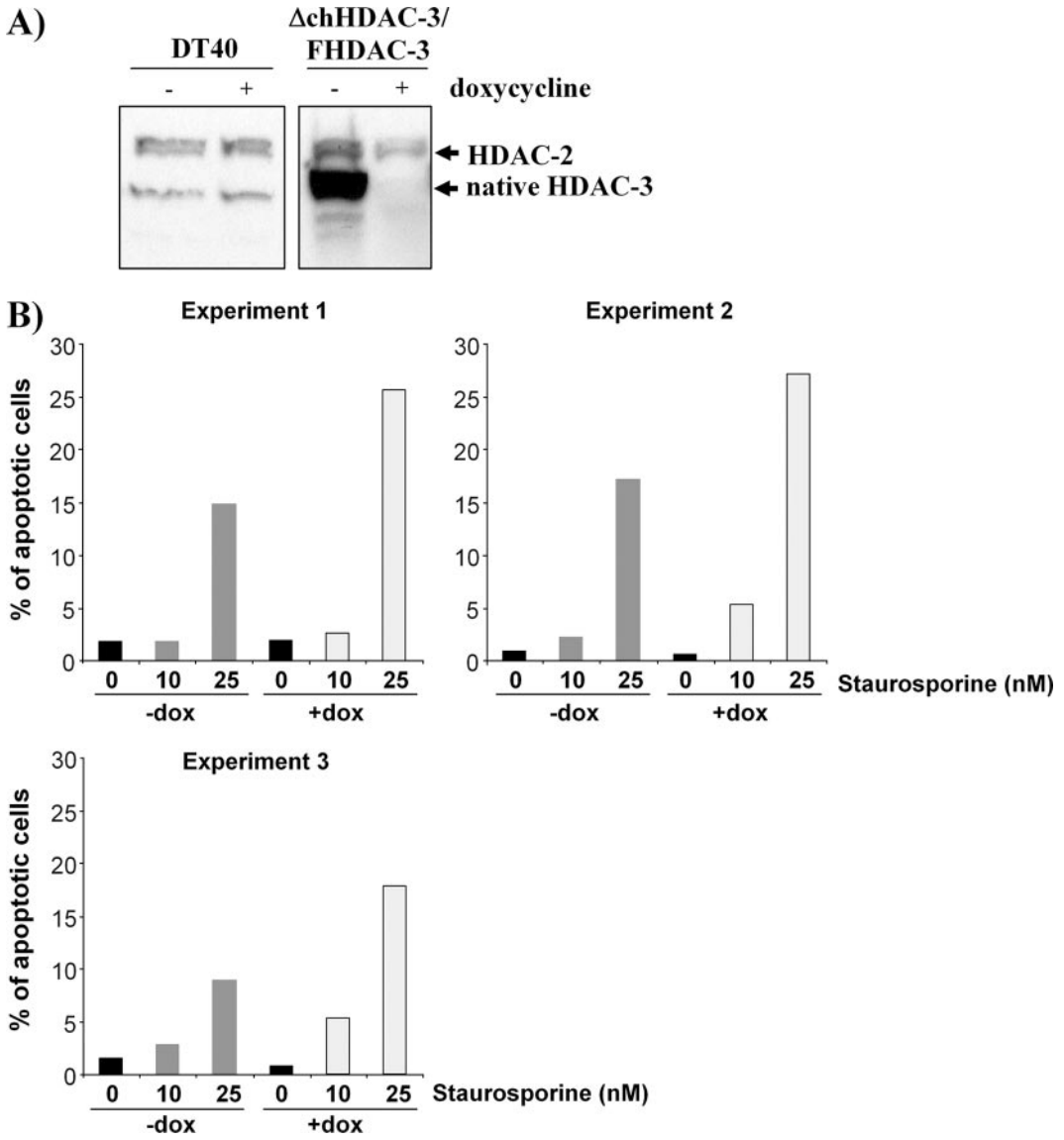

FIG. 5. HDAC-3 inhibition favors apoptosis. (A) DT40 (left) or DT40 ΔchHDAC-3/FHDAC-3 (right) cells were incubated or not incubated with doxycycline for 48 h in order to repress recombinant HDAC-3 expression. Total cell extracts were then analyzed by Western blotting using an anti-HDAC-3 antibody (from Transduction Laboratories, also recognizing chicken HDAC-2). −, absence of; +, presence of. (B) DT40 ΔchHDAC-3/FHDAC-3 cells were incubated with doxycycline (+dox) or not incubated with doxycycline (−dox) for 48 h in order to repress HDAC-3 expression. Cells were then treated or not treated with the indicated amount of staurosporine for 16 h. Apoptosis was measured by flow cytometry using an annexin V-FITC/7-AAD kit. Results from three entirely independent experiments are shown.

histone H4 (21, 52). We could not detect any major change in histone acetylation upon HDAC-3 knockdown (Fig. 7B), perhaps because siRNA knockdown was not efficient enough. We thus took advantage of the DT40 cells in which HDAC-3 expression can be fully inactivated (Fig. 5A). We found global histone H3 acetylation to be dependent on HDAC-3 expression (see Fig. S7 in the supplemental material). However, a comparison with the parental DT40 cells indicated that this result was due to a decrease of histone H3 acetylation induced by HDAC-3 overexpression in the absence of doxycycline rather than an increase of histone H3 acetylation in the absence of HDAC-3. Thus, HDAC-3 does not appear to be a major global histone deacetylase when expressed at endogenous levels. Alternatively, the loss of HDAC-3 can be fully compensated by another histone deacetylase. We also monitored histone acetylation following apoptosis induction, and we did not find any increase of histone acetylation (Fig. 7C). On the contrary, global acetylation on histone H3 or on histone H3 K9 strongly decreased in apoptotic cells, probably reflecting the inhibition of major HATs, such as CBP/p300 (37). Altogether, these results indicate that the apoptosis-dependent cleavage of HDAC-3 does not result in global histone hyperacetylation during apoptosis.

Analysis of HDAC-3 target genes. We thus investigated the effect of HDAC-3 cleavage on local histone acetylation. Indeed, local histone acetylation is known to correlate with tran-

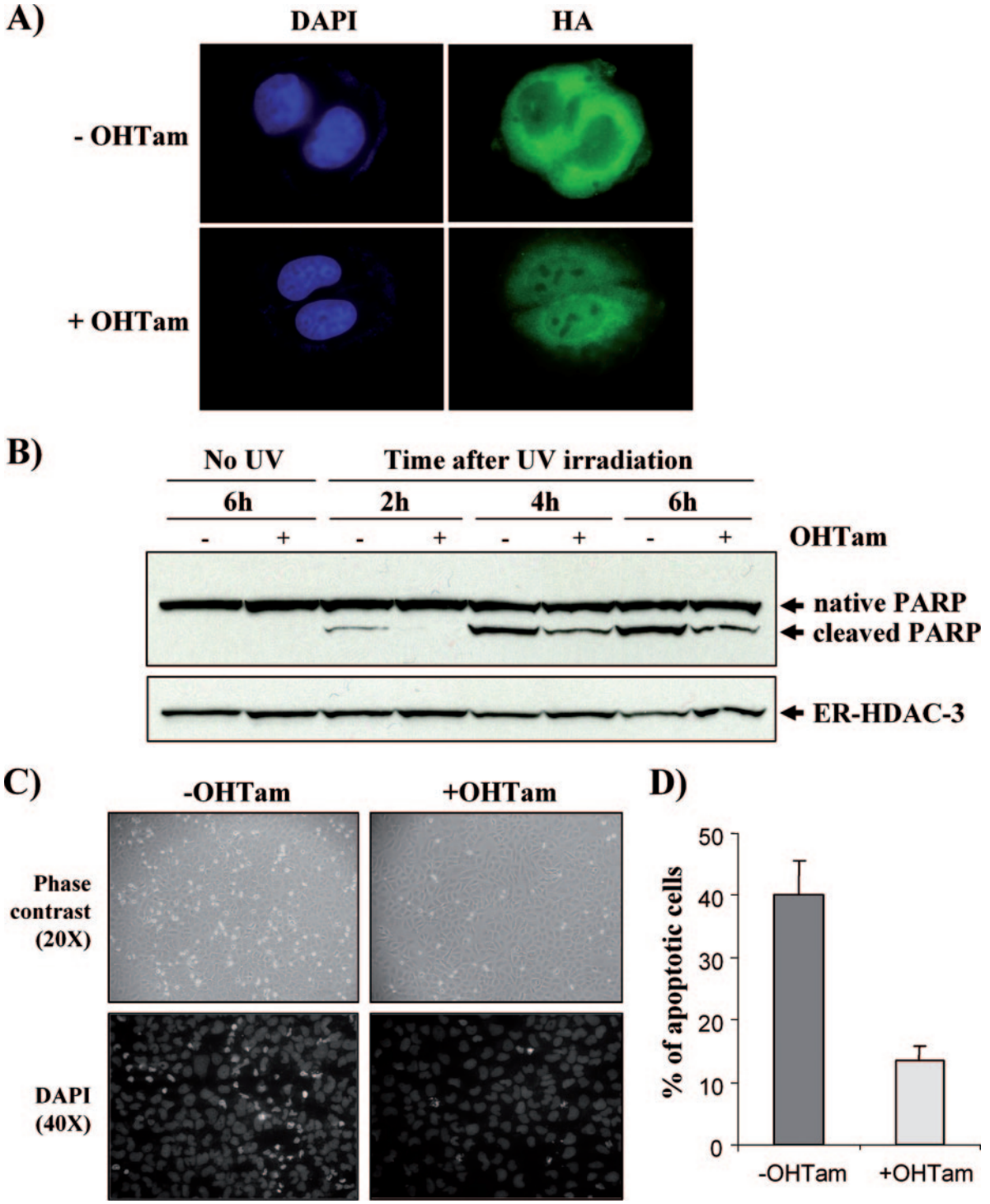

FIG. 6. Forced nuclear localization of HDAC-3 inhibits apoptosis. (A) U2OS R_{BHEN}^{HDAC-3} cells were plated on glass coverslips. Twenty-four hours later, cells were treated with 300 nM OHTam for 1 h and analyzed by immunofluorescence using an anti-HA antibody to detect the chimeric protein. DAPI staining was also used to visualize nuclei. (B) U2OS R_{BHEN}^{HDAC-3} cells that were treated or not treated with 300 nM OHTam for 1 h were UV irradiated (40 J/m^2) and then harvested after the indicated time. Total cell extracts were prepared and analyzed by Western blotting using anti-PARP antibody (upper panel) or anti-HA antibody ([lower panel] detecting the ER-HDAC-3 fusion protein). (C) U2OS R_{BHEN}^{HDAC-3} cells treated or not treated with 300 nM OHTam for 1 h were UV irradiated (40 J/m^2) and harvested after 6 h. A representative phase-contrast photograph and DAPI staining are shown. (D) Quantification of the experiment represented in panel C. One hundred cells were counted in three independent fields from each sample, and the percentage of cells harboring chromatin condensation (representative of apoptotic cells) was calculated. Error bars indicate standard deviations.

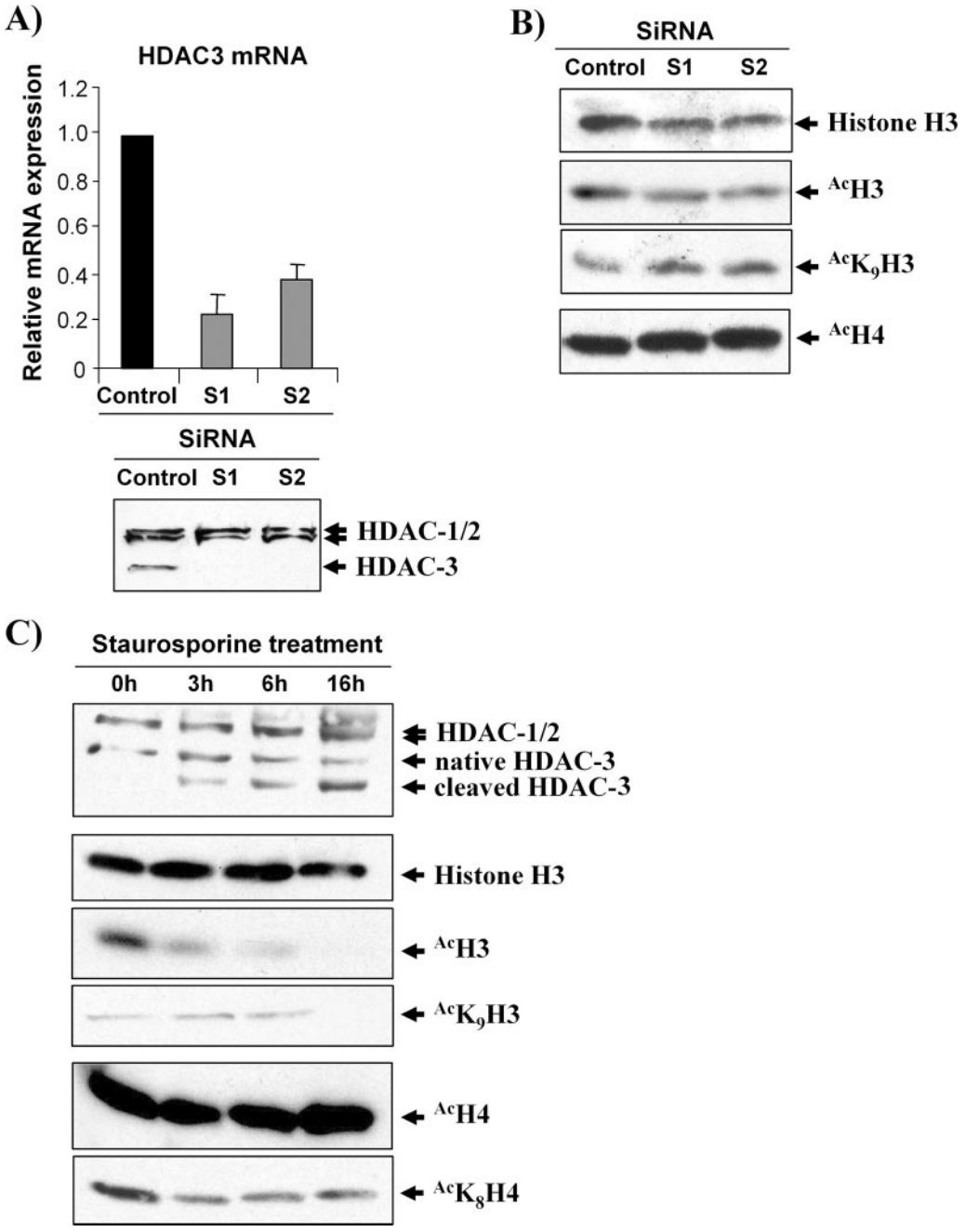

FIG. 7. HDAC-3 cleavage does not result in global histone hyperacetylation. (A) U2OS cells were transfected with the indicated siRNA (S1, anti-HDAC-3 S1; S2, anti-HDAC-3 S2). Forty-eight hours later, total RNA were extracted an reverse transcribed and the amounts of HDAC-3 and ribosomal phosphoprotein P0 cDNAs were measured by real-time PCR. Top panel represents the amount of HDAC-3 cDNA divided by the amount of P0 cDNA and calculated relative to 1 for cells transfected by the control siRNA. Total cell extracts were also prepared and subjected to anti-HDAC-3 Western blot analysis (bottom panel; the antibody from Transduction Laboratories also recognizes HDAC-1 and HDAC-2). Error bars indicate standard deviations. (B) U2OS cells were transfected with the indicated siRNA. Forty-eight hours following transfection, total cell extracts were prepared and analyzed by Western blotting using anti-total histone H3, anti-acetylated H3, anti-acetylated histone H3 K9, and anti-acetylated histone H4 antibodies. (C) U2OS cells were treated with 250 nM staurosporine for the indicated time. Total cell extracts were prepared and analyzed by Western blotting using anti-HDAC-3 (from Transduction Laboratories), anti-total histone H3, anti-acetylated H3, anti-acetylated histone H3 K9, anti-acetylated histone H4, and anti-acetylated histone H4 K8 antibodies.

scription and HDAC-3 has already been shown to mediate the transcriptional repression of specific genes through the local deacetylation of specific histone lysines. Thus, we reasoned that HDAC-3 cleavage and cytoplasmic relocalization could induce local histone acetylation and transcriptional activation of HDAC-3 target genes, including proapoptotic target genes. To characterize HDAC-3-target genes, we transfected U2OS cells with our siRNAs directed against HDAC-3 and analyzed

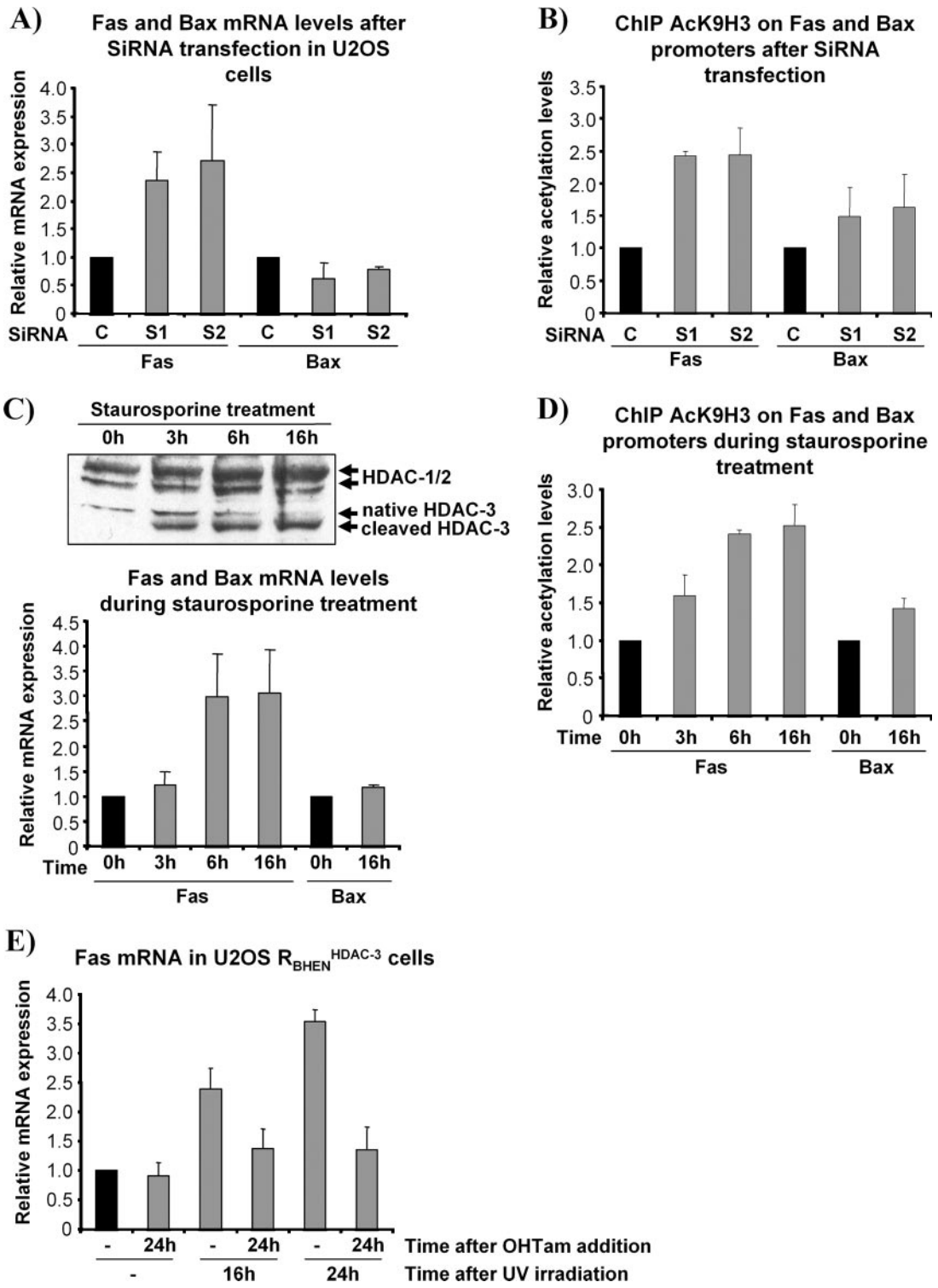

FIG. 8. The HDAC-3 target gene *fas* is activated during apoptosis. (A) U2OS cells were transfected with the indicated siRNA (S1, anti-HDAC-3 S1; S2, anti-HDAC-3 S2). Forty-eight hours following transfection, total RNAs were prepared and reverse transcribed and the amounts of *fas*, *bax*, and ribosomal phosphoprotein P0 cDNA were measured by real-time PCR. The amount of *fas* and *bax* cDNA was divided by the amount of P0 cDNA and calculated relative to 1 for cells transfected by the control siRNA. C, control. (B) U2OS cells transfected with the indicated siRNA were subjected 48 h later to a ChIP experiment using the anti-acetylated histone H3 K9 antibody. The amounts of immunoprecipitated *fas* or *bax* promoters or control GAPDH sequence were measured by real-time PCR and divided by the respective amounts present in the input. The results obtained for *fas* and *bax* promoters were then divided by that for GAPDH and calculated relative to 1 for cells transfected with the control siRNA. (C) U2OS cells were treated with 250 nM staurosporine for the indicated time. Cells were harvested, and HDAC-3 cleavage was monitored by anti-HDAC-3 Western blot analysis (upper panel). Total RNAs were also prepared, reverse transcribed, and analyzed as described for panel A. (D) U2OS cells treated with 250 nM staurosporine for the indicated time were subjected 48 h later to a ChIP experiment using the anti-acetylated histone H3 K9 antibody. Results were calculated as described for panel B. (E) U2OS R_{BHEN}^{HDAC-3} cells were treated (for 24 h) or not treated (−) with OHTam and irradiated (for 16 or 24 h) or not irradiated (−) with UV (10 J/m^2), as indicated. Total RNAs were prepared and reverse transcribed, and *fas* expression was analyzed as described for panel A. Results were calculated relative to 1 for untreated and unirradiated cells. Error bars indicate standard deviations.

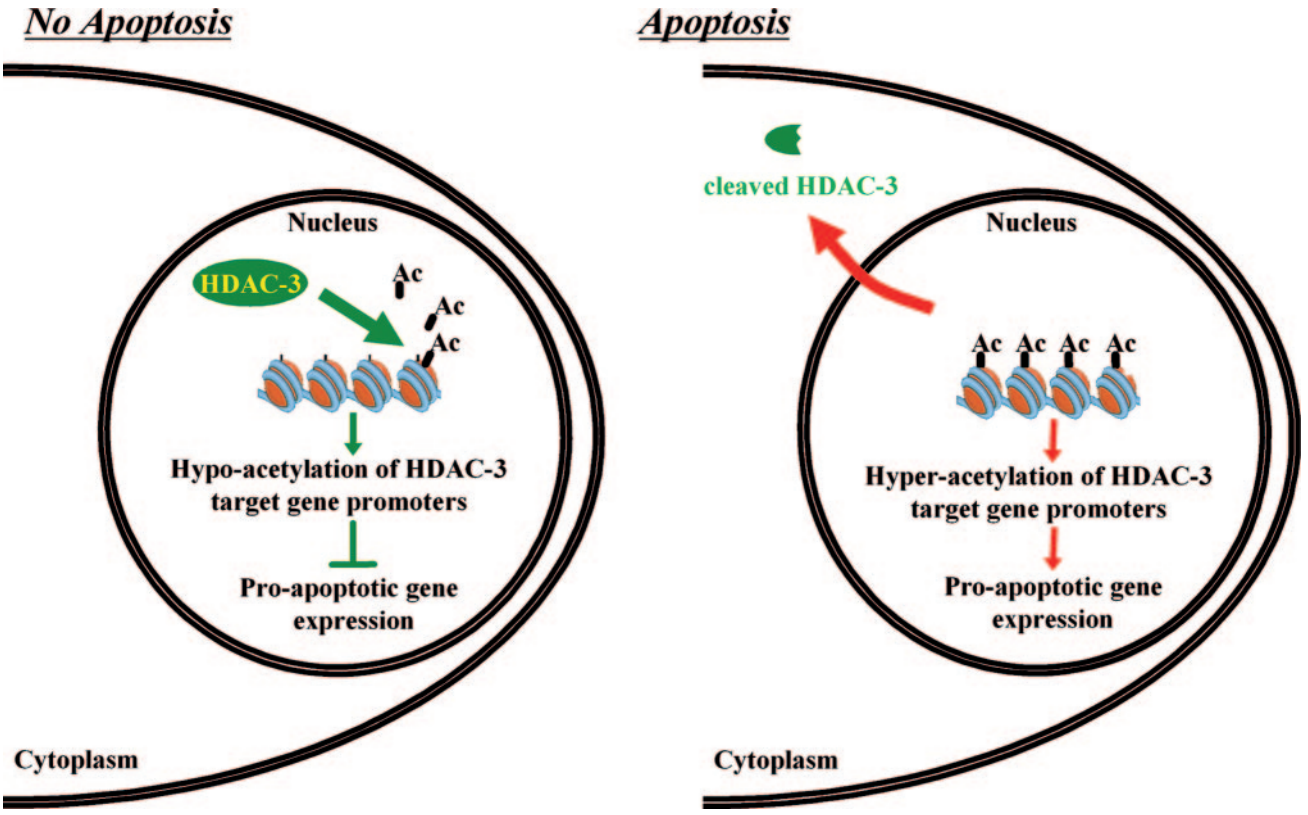

FIG. 9. Our working model. In unstressed cells (left panel), nuclear HDAC-3 represses its proapoptotic target promoters through histone deacetylation. When apoptosis is induced (right panel), HDAC-3 is cleaved and localizes in the cytoplasm. Therefore, histones on HDAC-3 target genes are no longer deacetylated, HDAC-3 repressive effects are relieved, and proapoptotic target genes are activated allowing further progression into apoptosis.

the expression of a number of proapoptotic genes by reverse transcription, followed by real-time PCR. Among the genes we tested, we reproducibly found that HDAC-3 knockdown using the two siRNAs led to the induction of the gene encoding the Fas receptor, whereas other proapoptotic genes, such as *bax*, were not affected (Fig. 8A). This result indicates that the *fas* gene is a specific target of HDAC-3. Moreover, by ChIP analysis, we found that upon HDAC-3 knockdown, the acetylation of histone H3 K9 increased on the *fas* promoter but not on the *bax* promoter (Fig. 8B). Since this lysine is a known target of HDAC-3 (52), this finding suggests that *fas* is a direct target of HDAC-3. We thus investigated whether this gene was activated when HDAC-3 was cleaved. We induced U2OS cells to enter apoptosis using staurosporine, and we analyzed the expression of the Fas-encoding gene by reverse transcription followed by real-time PCR. We observed a time-dependent increase in *fas* mRNA expression, concomitantly with the disappearance of full-length HDAC-3, whereas *bax* mRNA expression was unaffected even after 16 h of treatment (Fig. 8C). By ChIP, we also analyzed the acetylation of histone H3 K9 and we found that the acetylation on this lysine specifically increased on the *fas* promoter upon staurosporine treatment (Fig. 8D). The *fas* promoter escapes the global deacetylation of histone H3 K9 that we observed during apoptosis, probably because of local recruitment of a H3 K9-specific histone acetyltransferase. Altogether, these experiments demonstrate that HDAC-3 cleavage correlates with increased histone acetylation and the transcriptional activation of a target of HDAC-3, the *fas* promoter. Finally, we found that forced nuclear localization of HDAC-3 using ER-HDAC-3-expressing cells inhibited *fas* promoter activation upon UV irradiation (Fig. 8E), indicating that HDAC-3 cleavage and its consequent cytoplasmic relocalization is important for *fas* promoter activation during apoptosis.

DISCUSSION

In this work, we observed that HDAC-3 is cleaved following apoptosis induction. Our data point to the importance of this cleavage in the apoptotic process since (i) it is conserved from mammals to chicken, (ii) HDAC-3 expression inhibits apoptosis, (iii) HDAC-3 cleavage inactivates HDAC-3 activity towards nucleosomes through a change in its subcellular localization, and (iv) maintaining nuclear expression of HDAC-3 inhibits apoptosis. Our results thus uncover a new mechanism responsible for the control of proapoptotic genes during apoptosis induction (see our model in Fig. 9). In unstressed cells, HDAC-3 functions as a corepressor for many transcription factors involved in apoptosis, such as E2F (26), c-jun (47), peroxisome proliferator-activated receptor γ (12), and NF-κB (3, 15), and is known to repress the proapoptotic tumor necrosis factor-encoding gene (29). We demonstrate here that HDAC-3 is

also required for the repression of the Fas-encoding gene, although we do not know whether this repressive effect is direct since we failed to detect HDAC-3 binding to the *fas* promoter by ChIP (data not shown). Upon apoptosis induction, HDAC-3 is cleaved and cleaved HDAC-3 is localized in the cytoplasm and can no longer deacetylate histones on its proapoptotic target promoters. Histones on these promoters can now be hyperacetylated, thereby allowing the transcriptional activation of these proapoptotic genes and cell progression into apoptosis (Fig. 9). Although such a model is tempting, it is important to note that we cannot rule out the possibility that HDAC-3 cleavage changes something other than subcellular localization, such as enzymatic activity or interaction with cofactors or transcription factors. Indeed, as the ER-HDAC-3 fusion protein does not seem to be cleaved, it could function as a noncleavable mutant of HDAC-3.

Our results also raise the interesting possibility that cleaved HDAC-3 plays a role in the cytoplasm. Consistent with this possibility, cytoplasmic localization of HDAC-3 has already been observed (3, 16, 50). Moreover, lysine acetylation is a widespread posttranslational modification and many cytoplasmic proteins, such as γ-tubulin, are known to be acetylated (24). Since HDAC-3 can deacetylate proteins other than histones (6, 8, 42), cytoplasmic HDAC-3 could regulate the acetylation levels of a cytoplasmic protein and participate in cytoplasmic signal transduction pathways. Strikingly, the far C terminus of HDAC-3 is dispensable for its enzymatic activity (50), raising the possibility that cleaved HDAC-3 still possesses enzymatic activity. If this is the case, then cleaved HDAC-3 could participate in apoptosis through the deacetylation of a cytoplasmic protein since the apoptosis process is largely controlled through cytoplasmic events. Along this line, it would be interesting to investigate whether proteins of the mitochondrial apoptotic pathway are regulated by reversible acetylation. It has to be noted, however, that cytoplasmic localization of HDAC-3 by itself is not able to induce apoptosis (see our results in Fig. 6B, lane 1).

Another interesting question which derives from our data is whether HDAC-3 cleavage could be regulated. Indeed, given the importance of HDAC-3 cleavage in apoptosis induction (Fig. 6), this molecular event could be an important target of signaling pathways regulating apoptosis induction. Unfortunately, we do not know the enzyme responsible for HDAC-3 cleavage. We found that HDAC-3 cleavage is caspase dependent since it is inhibited by general caspase inhibitors and since it is not observed in cells mutated for the caspase-activating pathway (Fig. 2). Moreover, it is roughly concomitant with caspase activation since its kinetic is parallel to PARP cleavage (see Fig. S4 in the supplemental material). However, from our experiments, we cannot conclude that the cleavage is directly mediated by a caspase. Indeed, as also observed by others (34), in vitro cleavage of HDAC-3 by effector caspases was very inefficient (data not shown). Moreover, there is no consensus caspase site in the putative region of the cleavage. Thus, HDAC-3 cleavage is likely to be mediated by proteases other than caspases. Indeed, many proteases are activated in a caspase-dependent manner during the apoptotic process (23). Characterization of the protease(s) directly responsible for HDAC-3 cleavage is thus a major issue for understanding the determinants and the potential regulation of HDAC-3 cleavage.

Strikingly, maintaining nuclear HDAC-3 expression inhibited caspase-mediated PARP cleavage (Fig. 6B). Although we cannot rule out the possibility that this effect is due to the weak HDAC-3 overexpression obtained in the ER-HDAC-3-expressing cells, this result suggests that HDAC-3 cleavage is important for caspase activation. HDAC-3 cleavage would thus be downstream but also upstream of caspase activation: it will thus participate in a positive feedback loop, ensuring optimal caspase activation upon apoptosis induction. This is reminiscent of the caspase-dependent cleavage of the retinoblastoma protein Rb. Indeed, it was shown that abolishing Rb cleavage in mouse leads to the decrease in caspase activation upon apoptosis induction (5). Moreover, both HDAC-3 cleavage and Rb cleavage are thought to be involved in apoptosis by relieving the transcriptional repression of proapoptotic genes (the Fas-encoding gene [this study] and E2F1-dependent proapoptotic genes [13, 43], respectively). Altogether, these data point to the importance of caspase-dependent transcriptional activation of proapoptotic genes as a molecular mechanism for the caspase-activating positive regulatory loop.

Finally, our finding that HDAC-3 has an antiapoptotic function and that the inactivation of HDAC-3 may be important for apoptosis raises the question of the involvement of HDAC-3 in cancer. The overexpression of HDAC-3 was observed in carcinoma (35, 49), suggesting that cancer cells may have escaped apoptosis, at least in part, through HDAC-3 overexpression. Moreover, general histone deacetylase inhibitors are promising anticancer molecules which are currently under clinical trials. Because HDACs participate in many different various processes, drugs specifically targeting one or a subset of histone deacetylases may have fewer side effects than general inhibitors and are currently being actively searched (46). Our data suggest that HDAC-3-specific inhibitors may prove useful to induce apoptosis in cancer cells.

ACKNOWLEDGMENTS

We thank V. Régnier for help with DT40 culture; K. Helin and S. Müller for materials; L. Baricault for materials and helpful discussions; and C. Carron, T. Levade, and members of the D. Trouche's lab for helpful discussions.

This work was supported by a grant from the "Fondation de France" to D.T. F.E. was supported by fellowships from the "Ligue Nationale Contre le Cancer" and the "Fondation de France." O.V. was a recipient of a studentship from the "Ligue Nationale Contre le Cancer."

REFERENCES

1. **Ajiro, K.** 2000. Histone H2B phosphorylation in mammalian apoptotic cells. An association with DNA fragmentation. J. Biol. Chem. **275:**439–443.
2. **Allera, C., G. Lazzarini, E. Patrone, I. Alberti, P. Barboro, P. Sanna, A. Melchiori, S. Parodi, and C. Balbi.** 1997. The condensation of chromatin in apoptotic thymocytes shows a specific structural change. J. Biol. Chem. **272:**10817–10822.
3. **Baek, S. H., K. A. Ohgi, D. W. Rose, E. H. Koo, C. K. Glass, and M. G. Rosenfeld.** 2002. Exchange of N-CoR corepressor and Tip60 coactivator complexes links gene expression by NF-κB and beta-amyloid precursor protein. Cell **110:**55–67.
4. **Casciola-Rosen, L. A., G. J. Anhalt, and A. Rosen.** 1995. DNA-dependent protein kinase is one of a subset of autoantigens specifically cleaved early during apoptosis. J. Exp. Med. **182:**1625–1634.
5. **Chau, B. N., H. L. Borges, T. T. Chen, A. Masselli, I. C. Hunton, and J. Y. Wang.** 2002. Signal-dependent protection from apoptosis in mice expressing caspase-resistant Rb. Nat. Cell Biol. **4:**757–765.
6. **Chen, L.-F., W. Fischle, E. Verdin, and W. C. Greene.** 2001. Duration of nuclear NF-κB action regulated by reversible acetylation. Science **293:**1653–1657.
7. **Cheung, W. L., K. Ajiro, K. Samejima, M. Kloc, P. Cheung, C. A. Mizzen, A. Beeser, L. D. Etkin, J. Chernoff, W. C. Earnshaw, and C. D. Allis.** 2003. Apoptotic phosphorylation of histone H2B is mediated by mammalian sterile twenty kinase. Cell **113:**507–517.

8. **Chuang, H. C., C. W. Chang, G. D. Chang, T. P. Yao, and H. Chen.** 2006. Histone deacetylase 3 binds to and regulates the GCMa transcription factor. Nucleic Acids Res. **34:**1459–1469.
9. **Dhalluin, C., J. E. Carlson, L. Zeng, C. He, A. K. Aggarwal, and M. M. Zhou.** 1999. Structure and ligand of a histone acetyltransferase bromodomain. Nature **399:**491–496.
10. **Dignam, J. D., R. M. Lebowitz, and R. G. Roeder.** 1983. Accurate transcription initiation by RNA polymerase II in a soluble extract from isolated mammalian nuclei. Nucleic Acids Res. **11:**1475–1489.
11. **Eberharter, A., and P. B. Becker.** 2002. Histone acetylation: a switch between repressive and permissive chromatin. EMBO Rep. **3:**224–229.
12. **Fajas, L., V. Egler, R. Reiter, S. Miard, A. M. Lefebvre, and J. Auwerx.** 2003. PPARγ controls cell proliferation and apoptosis in an RB-dependent manner. Oncogene **22:**4186–4193.
13. **Fattman, C. L., S. M. Delach, Q. P. Dou, and D. E. Johnson.** 2001. Sequential two-step cleavage of the retinoblastoma protein by caspase-3/-7 during etoposide-induced apoptosis. Oncogene **20:**2918–2926.
14. **Fischle, W., F. Dequiedt, M. J. Hendzel, M. G. Guenther, M. A. Lazar, W. Voelter, and E. Verdin.** 2002. Enzymatic activity associated with class II HDACs is dependent on a multiprotein complex containing HDAC3 and SMRT/N-CoR. Mol. Cell **9:**45–57.
15. **Gao, Z., P. Chiao, X. Zhang, M. A. Lazar, E. Seto, H. A. Young, and J. Ye.** 2005. Coactivators and corepressors of NF-κB in IκBα gene promoter. J. Biol. Chem. **280:**21091–21098.
16. **Gao, Z., Q. He, B. Peng, P. J. Chiao, and J. Ye.** 2006. Regulation of nuclear translocation of HDAC3 by IκBα is required for tumor necrosis factor inhibition of peroxisome proliferator-activated receptor γ function. J. Biol. Chem. **281:**4540–4547.
17. **Glaser, K. B., J. Li, M. J. Staver, R. Q. Wei, D. H. Albert, and S. K. Davidsen.** 2003. Role of class I and class II histone deacetylases in carcinoma cells using siRNA. Biochem. Biophys. Res. Commun. **310:**529–536.
18. **Gray, S. G., A. H. Iglesias, B. T. Teh, and F. Dangond.** 2003. Modulation of splicing events in histone deacetylase 3 by various extracellular and signal transduction pathways. Gene Expr. **11:**13–21.
19. **Guenther, M. G., O. Barak, and M. A. Lazar.** 2001. The SMRT and N-CoR corepressors are activating cofactors for histone deacetylase 3. Mol. Cell. Biol. **21:**6091–6101.
20. **Guenther, M. G., W. S. Lane, W. Fischle, E. Verdin, M. A. Lazar, and R. Shiekhattar.** 2000. A core SMRT corepressor complex containing HDAC3 and TBL1, a WD40-repeat protein linked to deafness. Genes Dev. **14:**1048–1057.
21. **Hartman, H. B., J. Yu, T. Alenghat, T. Ishizuka, and M. A. Lazar.** 2005. The histone-binding code of nuclear receptor co-repressors matches the substrate specificity of histone deacetylase 3. EMBO Rep. **6:**445–451.
22. **Jacobson, R. H., A. G. Ladurner, D. S. King, and R. Tjian.** 2000. Structure and function of a human TAFII250 double bromodomain module. Science **288:**1422–1425.
23. **Johnson, D. E.** 2000. Noncaspase proteases in apoptosis. Leukemia **14:**1695–1703.
24. **Kouzarides, T.** 2000. Acetylation: a regulatory modification to rival phosphorylation? EMBO J. **19:**1176–1179.
25. **Kratzmeier, M., W. Albig, K. Hanecke, and D. Doenecke.** 2000. Rapid dephosphorylation of H1 histones after apoptosis induction. J. Biol. Chem. **275:**30478–30486.
26. **Lai, A., J. M. Lee, W. M. Yang, J. A. DeCaprio, W. G. Kaelin, Jr., E. Seto, and P. E. Branton.** 1999. RBP1 recruits both histone deacetylase-dependent and -independent repression activities to retinoblastoma family proteins. Mol. Cell. Biol. **19:**6632–6641.
27. **Li, J., J. Wang, Z. Nawaz, J. M. Liu, J. Qin, and J. Wong.** 2000. Both corepressor proteins SMRT and N-CoR exist in large protein complexes containing HDAC3. EMBO J. **19:**4342–4350.
28. **Littlewood, T. D., D. C. Hancock, P. S. Danielian, M. G. Parker, and G. I. Evan.** 1995. A modified oestrogen receptor ligand-binding domain as an improved switch for the regulation of heterologous proteins. Nucleic Acids Res. **23:**1686–1690.
29. **Mahlknecht, U., J. Will, A. Varin, D. Hoelzer, and G. Herbein.** 2004. Histone deacetylase 3, a class I histone deacetylase, suppresses MAPK11-mediated activating transcription factor-2 activation and represses TNF gene expression. J. Immunol. **173:**3979–3990.
30. **McLaughlin, F., and N. B. La Thangue.** 2004. Histone deacetylase inhibitors open new doors in cancer therapy. Biochem. Pharmacol. **68:**1139–1144.
31. **Milhas, D., O. Cuvillier, N. Therville, P. Clave, M. Thomsen, T. Levade, H. Benoist, and B. Segui.** 2005. Caspase-10 triggers Bid cleavage and caspase cascade activation in FasL-induced apoptosis. J. Biol. Chem. **280:**19836–19842.
32. **Mimnaugh, E. G., G. Kayastha, N. B. McGovern, S. G. Hwang, M. G. Marcu, J. Trepel, S. Y. Cai, V. T. Marchesi, and L. Neckers.** 2001. Caspase-dependent deubiquitination of monoubiquitinated nucleosomal histone H2A induced by diverse apoptogenic stimuli. Cell Death Differ. **8:**1182–1196.
33. **Narita, N., S. Fujieda, M. Tokuriki, N. Takahashi, H. Tsuzuki, T. Ohtsubo, and H. Matsumoto.** 2005. Inhibition of histone deacetylase 3 stimulates apoptosis induced by heat shock under acidic conditions in human maxillary cancer. Oncogene **24:**7346–7354.
34. **Paroni, G., M. Mizzau, C. Henderson, G. Del Sal, C. Schneider, and C. Brancolini.** 2004. Caspase-dependent regulation of histone deacetylase 4 nuclear-cytoplasmic shuttling promotes apoptosis. Mol. Biol. Cell **15:**2804–2818.
35. **Pilarsky, C., M. Wenzig, T. Specht, H. D. Saeger, and R. Grutzmann.** 2004. Identification and validation of commonly overexpressed genes in solid tumors by comparison of microarray data. Neoplasia **6:**744–750.
36. **Rogakou, E. P., W. Nieves-Neira, C. Boon, Y. Pommier, and W. M. Bonner.** 2000. Initiation of DNA fragmentation during apoptosis induces phosphorylation of H2AX histone at serine 139. J. Biol. Chem. **275:**9390–9395.
37. **Rouaux, C., N. Jokic, C. Mbebi, S. Boutillier, J. P. Loeffler, and A. L. Boutillier.** 2003. Critical loss of CBP/p300 histone acetylase activity by caspase-6 during neurodegeneration. EMBO J. **22:**6537–6549.
38. **Shimizu, M., A. Fontana, Y. Takeda, H. Yagita, T. Yoshimoto, and A. Matsuzawa.** 1999. Induction of antitumor immunity with Fas/APO-1 ligand (CD95L)-transfected neuroblastoma neuro-2a cells. J. Immunol. **162:**7350–7357.
39. **Smith, G. C., F. d'Adda di Fagagna, N. D. Lakin, and S. P. Jackson.** 1999. Cleavage and inactivation of ATM during apoptosis. Mol. Cell. Biol. **19:**6076–6084.
40. **Takami, Y., and T. Nakayama.** 2000. N-terminal region, C-terminal region, nuclear export signal, and deacetylation activity of histone deacetylase-3 are essential for the viability of the DT40 chicken B cell line. J. Biol. Chem. **275:**16191–16201.
41. **Talasz, H., W. Helliger, B. Sarg, P. L. Debbage, B. Puschendorf, and H. Lindner.** 2002. Hyperphosphorylation of histone H2A.X and dephosphorylation of histone H1 subtypes in the course of apoptosis. Cell Death Differ. **9:**27–39.
42. **Thevenet, L., C. Mejean, B. Moniot, N. Bonneaud, N. Galeotti, G. Aldrian-Herrada, F. Poulat, P. Berta, M. Benkirane, and B. Boizet-Bonhoure.** 2004. Regulation of human SRY subcellular distribution by its acetylation/deacetylation. EMBO J. **23:**3336–3345.
43. **Tsai, K. Y., Y. Hu, K. F. Macleod, D. Crowley, L. Yamasaki, and T. Jacks.** 1998. Mutation of E2f-1 suppresses apoptosis and inappropriate S phase entry and extends survival of Rb-deficient mouse embryos. Mol. Cell **2:**293–304.
44. **Tyteca, S., M. Vandromme, G. Legube, M. Chevillard-Briet, and D. Trouche.** 2006. Tip60 and p400 are both required for UV-induced apoptosis but play antagonistic roles in cell cycle progression. EMBO J. **25:**1680–1689.
45. **Vigo, E., H. Muller, E. Prosperini, G. Hateboer, P. Cartwright, M. C. Moroni, and K. Helin.** 1999. CDC25A phosphatase is a target of E2F and is required for efficient E2F-induced S phase. Mol. Cell. Biol. **19:**6379–6395.
46. **Wang, D. F., P. Helquist, N. L. Wiech, and O. Wiest.** 2005. Toward selective histone deacetylase inhibitor design: homology modeling, docking studies, and molecular dynamics simulations of human class I histone deacetylases. J. Med. Chem. **48:**6936–6947.
47. **Weiss, C., S. Schneider, E. F. Wagner, X. Zhang, E. Seto, and D. Bohmann.** 2003. JNK phosphorylation relieves HDAC3-dependent suppression of the transcriptional activity of c-Jun. EMBO J. **22:**3686–3695.
48. **Wen, Y. D., V. Perissi, L. M. Staszewski, W. M. Yang, A. Krones, C. K. Glass, M. G. Rosenfeld, and E. Seto.** 2000. The histone deacetylase-3 complex contains nuclear receptor corepressors. Proc. Natl. Acad. Sci. USA **97:**7202–7207.
49. **Wilson, A. J., D. S. Byun, N. Popova, L. B. Murray, K. L'Italien, Y. Sowa, D. Arango, A. Velcich, L. H. Augenlicht, and J. M. Mariadason.** 2006. HDAC3 and other class I HDACs regulate colon cell maturation and p21 expression, and are deregulated in human colon cancer. J. Biol. Chem.
50. **Yang, W. M., S. C. Tsai, Y. D. Wen, G. Fejer, and E. Seto.** 2002. Functional domains of histone deacetylase-3. J. Biol. Chem. **277:**9447–9454.
51. **Zhang, X., Y. Ozawa, H. Lee, Y. D. Wen, T. H. Tan, B. E. Wadzinski, and E. Seto.** 2005. Histone deacetylase 3 (HDAC3) activity is regulated by interaction with protein serine/threonine phosphatase 4. Genes Dev. **19:**827–839.
52. **Zhang, X., W. Wharton, Z. Yuan, S. C. Tsai, N. Olashaw, and E. Seto.** 2004. Activation of the growth-differentiation factor 11 gene by the histone deacetylase (HDAC) inhibitor trichostatin A and repression by HDAC3. Mol. Cell. Biol. **24:**5106–5118.